第28卷 第4期
2007年4月

半 导 体 学 报
CHINESE JOURNAL OF SEMICONDUCTORS

Vol.28 No.4
Apr.,2007

Observation of Dislocation Etch Pits in GaN Epilayers by Atomic Force Microscopy and Scanning Electron Microscopy*

Gao Zhiyuan†, Hao Yue, Zhang Jincheng, Zhang Jinfeng, Chen Haifeng, and Ni Jinyu

(*Institute of Microelectronics, Xidian University, Xi'an 710071, China*)

Abstract: A combination of atomic force microscopy (AFM) and scanning electron microscopy (SEM) is used to characterize dislocation etch pits in Si-doped GaN epilayer etched by molten KOH. Three types of etch pits with different shapes and specific positions in the surface have been observed, and a model of the etching mechanism is proposed to explain their origins. The pure screw dislocation is easily etched along the steps that the dislocation terminates. Consequently a small Ga-polar plane is formed to prevent further vertical etching, resulting in an etch pit shaped like an inverted truncated hexagonal pyramid at the terminal chiasma of two surface steps. However, the pure edge dislocation is easily etched along the dislocation line, inducing an etch pit of inverted hexagonal pyramid aligned with the surface step. The polarity is found to play an important role in the etching process of GaN.

Key words: KOH etching; dislocation; GaN; polarity
PACC: 6170J; 7280E
CLC number: O77+2 **Document code**: A **Article ID**: 0253-4177(2007)04-0473-07

1 Introduction

Wet etching techniques are extensively used for defect evaluation due to the merits of low cost and simple experimental procedure.[1] The shape of etch pits is well correlated with the type of defects, and the etch-pit density (EPD) may correspond to the density of defects. However, as far as GaN is concerned, the density, types and distribution of defects can vary significantly with different growth-related conditions, and hence there is considerable discrepancy in the literature about the origins of the etch pits.

Generally speaking, there are two ways to investigate the relationship between the etch-pits and the threading dislocations: direct observation and indirect quantitative comparison. Cross-sectional TEM works for the first way. In this way, Kenji *et al*.[2] found all the etch pits corresponding to mixed dislocations, while Hino *et al*.[3] observed that both the screw and mixed dislocations terminated at the bottom of the etch pits. Another direct technique is plane-view TEM, by which Weyher *et al*.[4] found etch pits formed on nanotube and mixed dislocations, while Hong *et al*.[5,6] concluded that only nanotube can cause the etch pits. However, pure edge dislocations related with the etch pits cannot be found through direct observation, due to the small sampling area of TEM and the difficulties in sample preparation.

Indirect quantitative comparison means comparing EPD with dislocation densities obtained by other test techniques such as TEM and X-ray diffraction (XRD). This method produces more discrepancies than direct observation due to the existence of more uncertainties in the measurements for comparison. For instance, Visconti *et al*.[7~10] and Xu *et al*.[11] found that the total dislocation density obtained by TEM was close to the EPD, while Takahiro *et al*.[12] found that the EPD was smaller than the dislocation density. Yamamoto *et al*.[13] compared the EPD with the dark spot density of the electron beam induced current (EBIC), and found that different pit sizes corresponded to different dislocation types.

In this paper, we propose another way to identify the origins of the etch pits in our sample. By a thorough analysis of the small details provided by SEM and AFM, the 3D shapes of the etch

* Project supported by the State Key Development Program for Basic Research of China (Nos. 2002CB3119, 513270407) and the National Defense Scientific and Technical Key Laboratory Fund of China (Nos. 51432030204DZ0101, 51433040105DZ0102)

† Corresponding author. Email: gaodemailbox@126.com

Received 23 October 2006, revised manuscript received 28 November 2006

©2007 Chinese Institute of Electronics

pits as well as their specific positions can be obtained. The proposed model of etching process can explain the result well. In addition, X-ray experiments were performed to confirm this proposal.

2 Experiment

The Si-doped n-type GaN film used in this paper was grown on (0001)-sapphire substrates with low-temperature (LT) GaN buffer in an MOCVD reactor using ammonia (NH_3), trimethylgallium (TMGa), and SiH_4 as precursors. The thickness of the GaN layers was 1094nm. The electron concentration was $1.49 \times 10^{18} cm^{-3}$, and the mobility was $83.74 cm^2/(V \cdot s)$ according to Hall measurements.

Etching was performed in molten KOH for times of 1,2,3,5,8, and 10min at 210 and 236℃, respectively. The etchant was heated in a nickel crucible on a hot-plate. The temperature was monitored using a pt100 immersed in the etchant with accuracy within 5℃. After the etchant reached the specified temperature, the GaN sample was immersed in the etchant for a specified time, and then immediately taken out to halt etching.

A high-resolution field-effect scanning electron microscope (JEOL 7400F) was used to get a clear SEM image. AFM observations were carried out with a Shimadzu Instruments SPM-9500 J3 in tapping mode. The probe radius was about 5nm. XRD measurements were performed on a Phillips X' Pert PRO MRD system using CuKα radiation.

3 Results

3.1 Three types of etch pits observed by SEM and AFM

Figure 1 (a) shows a typical SEM image of the Si-doped GaN surface etched in molten KOH at 210℃ for 5min. Three types of well-defined hexagonal etch pits, marked "α", "β", and "γ", are observed. In order to see them clearly, we have magnified some images and made a schematic illustration for each, as shown in Figs. 1 (b), (c), and (d). According to the topographic contrast principle of the secondary electron image,[14] the brightest part represents a steep incline, the gray area should be a plane or a gentle incline, and the black core means there is a hole or a sharp groove. Therefore, the α type etch pit may be an inversed truncated hexagonal pit, and the β type an inversed hexagonal pyramid, while the γ type is not that clear. The following AFM observation confirms the results for types α and β, and makes clear the shape of the γ type etch pit.

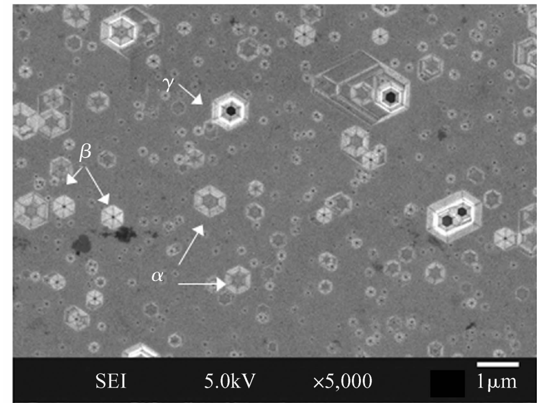

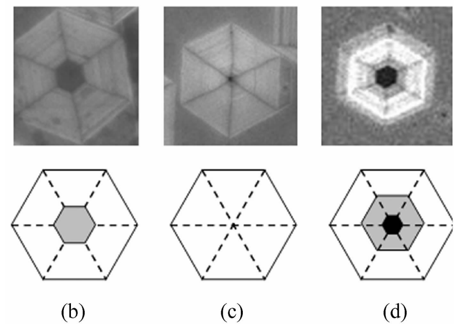

Fig. 1 SEM image of KOH etched GaN film surface (a), α type (b), β type (c), and γ type (d) etch pits and their corresponding schematic views

The AFM observation in Fig. 2 (a) shows an image of a stepped/terrace structure with an average step height of 0.25nm, which is consistent with the height expected for a Ga-N bilayer on a (0001) GaN surface. The white spots in the image are contaminants. At the lower right of the image is a hexagonal etch pit terminated by two surface steps. The depth is measured along three lines across it in three symmetry axes of the hexagon, marked by AB, CD and EF in the image to indicate the three corresponding line profiles shown below the image. This trapezoidal profile confirms that the α type etch pit is an inversed truncated

hexagonal pyramid, as schematically shown in Fig. 3 (a). In the same way, the pit selected in Fig. 2 (b) is a β type etch pit for the triangular profile, and its 3D schematic view is shown in Fig. 3 (b). Note that this type tends to arrange along the surface step line, instead of terminating two surface steps.

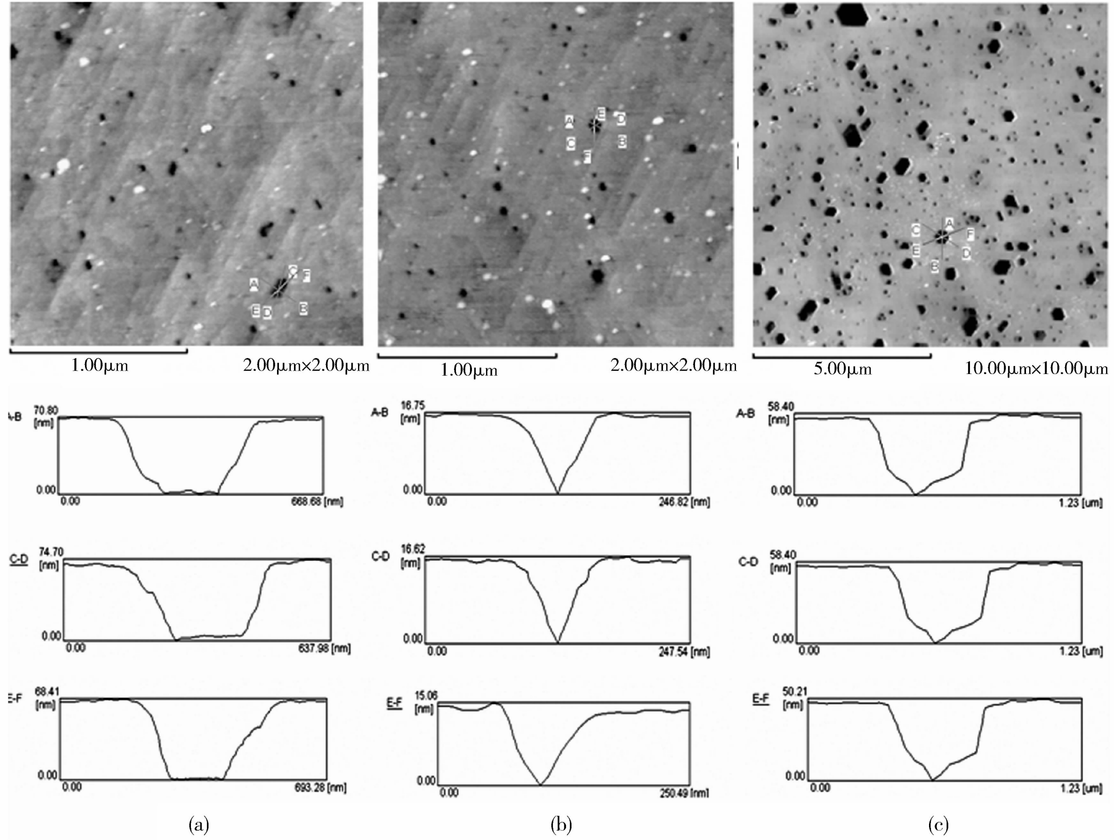

Fig. 2　Typical AFM images of KOH etched GaN film surface　The etch pits selected to perform line profile in each image are respectively: (a) α type; (b) β type; (c) γ type. The lines labeled AB, CD and EF across the pit indicate three corresponding line profiles shown below each AFM image.

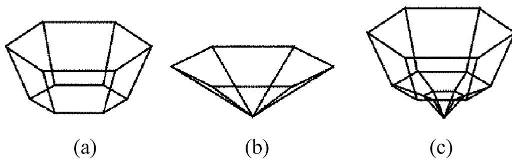

Fig. 3　3D schematic views of α type (a), β type (b), and γ type (c) etch pits

The profile of the pit selected in Fig. 2 (c) has a combination of triangular and trapezoidal shapes, which seems to be the result of a combination of α and β types. The steep incline corresponds to the brightest area in the SEM image, and the gentle incline corresponds to the gray area. The triangular groove at profile bottom should correspond to the hexagonal black core in the SEM image for the following three reasons: first, the width of the triangular groove is comparable with the radius of the black core of some γ type pits in SEM image; second, the black core is much wider than the radius of the AFM probe, so the profile of a hole should look like a very deep well, but not a triangular groove as observed; third, the groove, though not very sharp, is deep in the bottom, and thus its secondary electron is still unlikely to be collected. Consequently, it can be concluded that the profiled pit in this figure should be a γ type etch pit.

In summary, high-resolution field-effect SEM is superior in getting a good visual plane-view image of etch pits as well as having a large sampling area in comparison with other techniques, including TEM. AFM is able to give us information in

the vertical direction and the specific positions of the etch pits. A combination of the two methods helps to distinguish the etch pit's shape, which also provides an easy way to identify different dislocation densities.

3.2 An etching mechanism model to identify etch pit origin

It is believed that α type etch pits could be correlated with pure screw dislocations. A screw dislocation creates a step when it ends up at the surface[15,16], as shown in Fig. 4 (a). This step will associate with the natural surface terrace structure. It can be proved by the AFM results that α type etch pits terminate surface steps, as shown in Fig. 2 (a). In the beginning, etching can form a few ascending spiral steps, as shown in Fig. 4 (b). These spiral steps are so vulnerable that they will soon be attacked by OH^{-1} through further etching, and only a small plane facet will be left, as shown in Fig. 4 (c). This small facet must be Ga-terminated. Even if it were N-terminated, it would be further etched to become Ga-terminok due to the chemical stabilization of Ga-face[17~21]. Once this small smooth plane is formed, the vertical etching velocity will become rather smaller than the transverse one, and finally this small plane will turn into a big one which can be observed by microscopy. Thus the screw dislocation can be etched to form an inversed truncated pyramid at the surface steps' terminal chiasma.

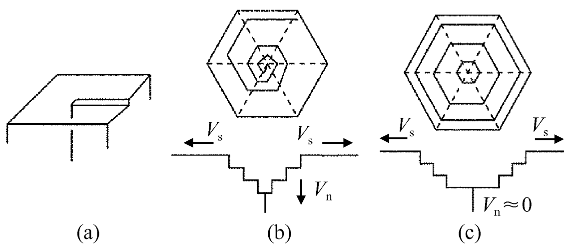

Fig.4 (a) Surface termination of a pure screw dislocation; (b) A few spiral steps formed at the initial stage of etching; (c) Formation of small Ga-face to prevent further vertical etching

It is believed that β type etch pits correspond to pure edge dislocations. Figure 5 (a) illustrates a pure edge dislocation with a burgers vector $\boldsymbol{b} = 1/3[11\bar{2}0]$, and "×" denotes the edge dislocation line, which is vertical to the surface. Since each atom in this line has a dangling bond, they are the most vulnerable to attack. There is little chance that a small Ga-terminated facet will form to prevent vertical etching as in the case of screw dislocation. Thus the pure edge dislocation can be etched to form an inversed pyramid. As the γ type is a combination of α and β types, it can be associated with a mixed dislocation.

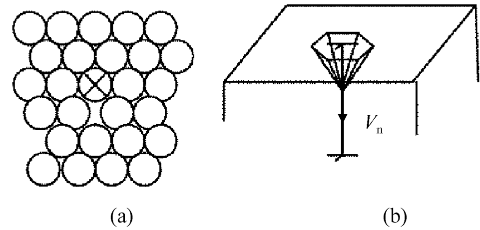

Fig.5 (a) Illustration of a pure edge dislocation; (b) Etching is easier to carry on along the vertical dislocation line

In summary, the difference in etch pit shapes between a pure screw and a pure edge dislocation lies in the fact that etching the former depends more on the surface steps associated with the dislocation, while etching the latter depends more on the dangling bonds along the dislocation line. What should be emphasized is that the chemical stabilization of the Ga-polar surface plays an important part in etch pit formation.

3.3 EPD and dislocation densities

By counting etch pits of different shapes in the FESEM images, the densities of α, β, and γ type etch pits can be easily determined to be 3.0×10^7, 4.4×10^8, and $6.7\times10^6 cm^{-2}$, respectively. In order to avoid nonuniform distribution of dislocations, several images of different sampling areas are needed to get an average value. The density of β type etch pits is about one order larger than that of α type, and about two orders larger than that of γ type. It should be pointed out that for the purpose of clearly showing as many as possible of all three types of etch pits in one image, the densities of α, β, and γ type pits in Fig. 1 (a) are approximately equal. However, the density ratio in Fig. 6 (a) is the actual one.

In order to check the accuracy of this proposal, X-ray rocking curves of (0002) and $(30\bar{3}2)$ reflections were recorded, since the (0002) diffraction peak broadening is related to the mean tilt

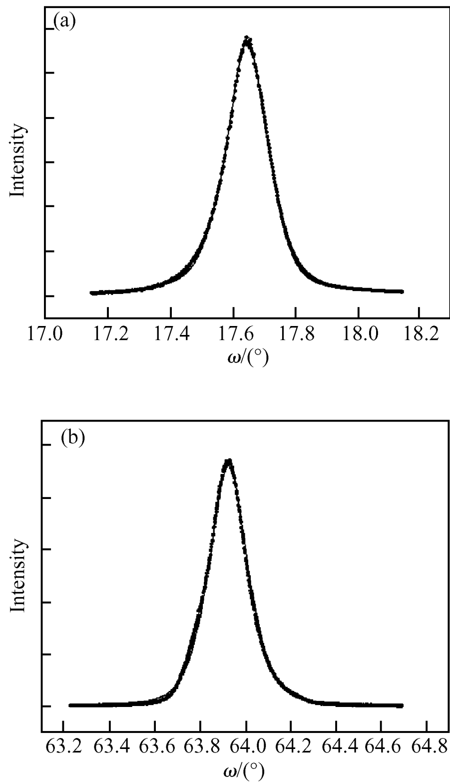

Fig.6 Measured rocking curves of (0002) reflection (a) and $(30\overline{3}2)$ reflection (b), as well as the fitted curves using a function of Pseude-Voigt The dotted lines are experimental data and the lines are fitted to them.

angle of the mosaic structure[22] induced by screw dislocations[23,24], and the $(30\overline{3}2)$ peak broadening can be taken as an appropriate figure of merit for the twist[25,26] induced by edge dislocations [23,24]. It should be pointed out that the broadening of the XRD curve is not affected only by the dislocation structure. Fortunately, however, wafer bending and heterogeneous strain do not influence it, due to the small acceptance angle of the detector[27]. In addition, both the intrinsic width of the reflection for the crystal and the instrumental broadening is negligible[25]. Hence a separation analogous to the Pseudo-Voigt function can be performed to obtain the correlation length parallel to the substrate surface and the angular rotation at the dislocations[27,28], and the dislocation densities can be obtained using the equation[29]:

$$N = \frac{\alpha}{2.1|\boldsymbol{b}|L_{/\!/}} \qquad (1)$$

where α is the rotation angle, $L_{/\!/}$ is the lateral correlation length, and $|\boldsymbol{b}| = 0.5185\text{nm}$ for the screw dislocation and $|\boldsymbol{b}| = 0.3189\text{nm}$ for the edge dislocation. As shown in Fig. 6, the fitted curves agree quite well with the measured rocking curves of (0002) and $(30\overline{3}2)$ reflections. The calculated dislocation densities are $5.06 \times 10^8 \text{cm}^{-2}$ for edge dislocations and $6.72 \times 10^7 \text{cm}^{-2}$ for screw dislocations. It can be seen that β type EPD is approximate to the edge dislocation density, and the total EPD of α and γ type is approximate to the screw dislocation density, since XRD cannot distinguish between pure screw and mixed dislocation.

4 Discussion

The above-mentioned model is partly in agreement with the results of some literature. Kapolnek *et al*.[30] reported that AFM measurements showed a step termination density in close agreement with TEM measurements of screw and mixed threading dislocation density. Kenji[2] found that the etch pit positioned at surface step termination revealed by AFM corresponded to the surface termination of pure-screw or mixed dislocations as observed by TEM.

If these three types of etch pits evolve from one type with time, then their diameters should be correlated to their designation, for instance, β pit diameters <α pit diameters <γ pit diameters, and after being etched both for a short time (or at a low temperature) and for a long time (or at a high temperature), there should be only one type of etch pit. However, such orderliness cannot be found in all of our etched samples. As shown in Fig. 7 (a), diameters of α type etch pits can be larger or smaller than those of β type. The small etch pits hidden in the background in Fig. 1 (a), which should be newly formed pits, have features similar to the larger ones, as shown in Fig. 7 (b). All of the three shapes of the etch pits can be found in the film surface etched under a mild condition, i.e. with a short time or a low temperature. For example, Figure 7 (c) shows the surface morphology of GaN etched for 2min at 210℃. The large etch pit on the left of the image is γ type, and the other two large pits on the right are α type. When overetching, i. e. etching for a long time or at a high temperature, all the three shapes can also be found, as shown in Fig. 7 (a).

The smaller EPD compared with the dislocation density observed by TEM presented in some

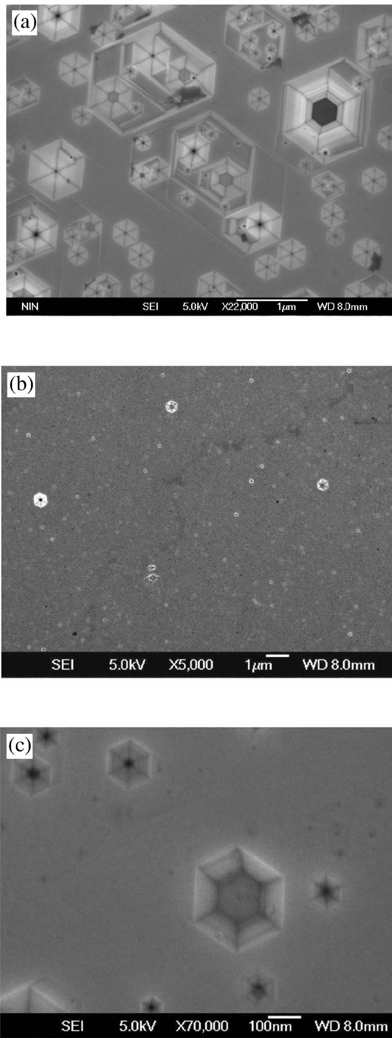

Fig. 7 (a) SEM images of a slightly overetched GaN film surface, some etch pits begin to merge together; (b) Typical surface morphology etched under a mild condition; (c) Part of the image in Fig. 1 (a) over a larger magnification

literature[12,31] is supposed to be the result of insufficient etching, in which case dislocation etch pits have not got enough time to form, or are too small to be observed. As can be seen in Fig. 7 (c), it is too difficult to count the smaller pits hidden in the background. However, one can count the small pits from an image with larger magnification, but charging effect and uniformity introduce other problems. Therefore, a reasonable over-etching is needed in order to fully reveal the defects so that they can be easily identified and counted.

5 Conclusion

Three etch pit types in KOH-etched Si-doped GaN surface have been observed by a combination of atomic force and scanning electron microscopy, and a model of the etching mechanism is proposed to identify their origins. Polarity is found to play an important part in the etch pit formation, which is truly an amazing point of this compound material.

References

[1] Zhuang D, Edgar J H. Wet etching of GaN, AlN, and SiC: a review. Mater Sci Eng R, 2005, 48: 1

[2] Shiojima K. Atomic force microscopy and transmission electron microscopy observation of KOH etched GaN surfaces. J Vac Sci Technol B, 2000, 18(1): 37

[3] Hino T, Tomiya S, Miyajima T, et al. Characterization of threading dislocation in GaN epitaxial layers. Appl Phys Lett, 2000, 72: 3421

[4] Weyher J L, Brown P D, Rouviere J L, et al. Recent advances in defect-selective etching of GaN. J Cryst Growth, 2000, 210: 151

[5] Hong S K, Kim B J, Park H S, et al. Evaluation of nanopipes in MOCVD grown (0001) GaN/Al_2O_3 by wet chemical etching. J Cryst Growth, 1998, 191: 275

[6] Hong S K, Yao T, Kim B J, et al. Origin of hexagonal shaped etch pits formed in GaN films. Appl Phys Lett, 2000, 77(1): 82

[7] Visconti P, Jones K M, Reshchikov M A, et al. Dislocation density in GaN determined by photoelctrochemical and hot wet etching. Appl Phys Lett, 2000, 77: 3532

[8] Visconti P, Huang D, Reshchikov M A, et al. Investigation of defects and polarity in GaN using hot wet etching AFM TEM and convergent beam electron diffraction. Phys Status Solidi B, 2001, 228(2): 513

[9] Visconti P, Huang D, Yun F, et al. Rapid delineation of extended defects in GaN and a novel method for their reduction. Phys Status Solidi A, 2002, 190(1): 5

[10] Visconti P, Huang D, Reshchikov M A, et al. Investigation of defects and surface polarity in GaN using hot wet etching together with microscopy and diffraction techniques. Mater Sci Eng B, 2002, 93: 229

[11] Xu X, Vaudo R P, Flynn J, et al. Acid etching for accurate determination of dislocation density in GaN. J Electron Mater, 2002, 31(5): 402

[12] Kozawa T, Kachi T, Ohwaki T, et al. Dislocation etch pits in GaN epitaxial layers grown on sapphire substrates. J Electrochem Soc, 1996, 143(1): L17

[13] Yamamoto K, Ishikawa H, Egawa T, et al. EBIC observation of n-GaN grown on sapphire substrates by MOCVD. J Cryst Growth, 1998, 189/190: 575

[14] Zhou Yu, Wu Gaohui. Material analysis and test techniques. Harbin: Harbin Institute of Technology, 2004 (in Chinese) [周玉, 武高辉. 材料分析测试技术. 哈尔滨: 哈尔滨工业大学出版社, 2004]

[15] Hull D, Bacon D J. Translated by Ding Shushen, Li Qi. Introduction to dislocations. Beijing: Science Press, 1990 (in Chinese) [Hull D, Bacon D J, 著. 丁树深, 李齐, 译. 位错导论. 北京: 科学出版社, 1990]

[16] Friedel J. Translated by Wang Yu. Dislocations. Beijing: Science Press, 1980 (in Chinese) [Friedel J,著.王煜,译.位错.北京:科学出版社,1980]

[17] Huang D, Visconti P, Jones K M A, et al. Dependence of GaN polarity on the parameters of the buffer layer grown by MBE. Appl Phys Lett, 2001, 78: 4145

[18] Palacios T, Calle F, Varela M, et al. Wet etching of GaN grown by molecular beam epitaxy on Si(111). Semicond Sci Technol, 2000, 15: 996

[19] Li D, Sumiya M, Yoshimura K, et al. Characteristics of the GaN polar surface during an etching process in KOH solution. Phys Status Solidi A, 2000, 180: 357

[20] Li D, Sumiya M, Fuke S, et al. Selective etching of GaN polar surface in potassium hydroxide solution studied by X-ray photoelectron spectroscopy. J Appl Phys, 2001, 90: 4219

[21] Kim B J, Lee J W, Park H S, et al. Wet etching of (0001) GaN/Al_2O_3 grown by MOVPE. J Electron Mater, 1998, 27(5): L32

[22] Baia J, Wanga T, Parbrooka P J, et al. A study of dislocations in AlN and GaN films grown on sapphire substrates. J Cryst Growth, 2005, 282: 290

[23] Sun Y J, Brandt O, Liu T Y, et al. Determination of the azimuthal orientational spread of GaN films by X-ray diffraction. Appl Phys Lett, 2002, 81(26): 4928

[24] Fantner E B, Ryan T, Schurman M, et al. XRD and optical characterization of GaN and associated substrate materials. Materials Science Forum, 2000, 321～324: 1056

[25] Heinke H, Kirchner V, Einfeldt S, et al. X-ray diffraction analysis of the defect structure in epitaxial GaN. Appl Phys Lett, 2000, 77(14): 2145

[26] Zheng X H, Chen H, Yan Z B. Determination of twist angle of in-plane mosaicspread of GaN films by high-resolution X-ray diffraction. J Cryst Growth, 2003, 255: 63

[27] Metzger T, Hopler R, Born E, et al. Defect structure of epitaxial GaN films determined by transmission electron microscopy and triple-axis X-ray diffractometry. Philosophical Magazine A, 1998, 77(4): 1013

[28] De Keijser Th H, Mittemeijer E J, Rozendaal H C F. The determination of crystallite size and lattice strain parameters in conjunction with the profile refinement method for the determination of crystal structures. J Appl Cryst, 1983, 16: 309

[29] Hordon M J, Averbach B L. X-ray measurements of dislocation density in deformation copper and aluminum single crystals. Acta Metal, 1961, 9: 237

[30] Kapoinek D, Wu X H, Heying B, et al. Structural evolution in epitaxial metalorganic chemical vapor deposition grown GaN films on sapphire. Appl Phys Lett, 1995, 67(11): 1541

[31] Lu Min, Chang Xin, Fang Huizhi, et al. Etch-pits of GaN films with different etching methods. Chinese Journal of Semiconductors, 2004, 25: 1376

用原子力显微镜和扫描电镜研究GaN外延层中的位错腐蚀坑*

高志远† 郝 跃 张进城 张金凤 陈海峰 倪金玉

(西安电子科技大学微电子研究所，西安 710071)

摘要： 用原子力显微镜和扫描电镜相结合的方法表征了KOH腐蚀后的Si掺杂GaN外延层中的位错腐蚀坑.根据腐蚀坑的不同形状和在表面的特定位置可将其分成三种类型,它们的起源可由一个关于腐蚀机制的模型加以解释.纯螺位错易于沿着由它结束的表面阶梯被腐蚀,形成一个小的Ga极性面以阻止进一步的纵向腐蚀,因而其腐蚀坑是位于两个表面阶梯交结处的截底倒六棱椎.纯刃位错易于沿位错线被腐蚀,因而其腐蚀坑是沿着表面阶梯分布的尖底倒六棱椎.极性在GaN的腐蚀过程中起了重要作用.

关键词： KOH腐蚀；位错；GaN；极性

PACC： 6170J；7280E

中图分类号： O77+2　　**文献标识码：** A　　**文章编号：** 0253-4177(2007)04-0473-07

* 国家重大基础研究发展计划（批准号：2002CB3119，513270407）及国防科技重点实验室基金（批准号：51432030204DZ0101，51433040105DZ0102）资助项目

† 通信作者.Email:gaodemailbox@126.com

2006-10-23收到,2006-11-28定稿

©2007 中国电子学会